Continuum Mech. Thermodyn. (2002) 14: 231–239
Digital Object Identifier (DOI) 10.1007/s001610200088

Original Article

Complex backflow dynamics in nematic liquid crystals†

D. Svenšek⋆, S. Žumer

Oddelek za fiziko, Fakulteta za matematiko in fiziko, Univerza v Ljubljani, Jadranska 19, 1000 Ljubljana, Slovenija

Received December 31, 2001 / Published online May 21, 2002 –
Communicated by Epifanio Virga, Pavia

The backflow problem of a nematic liquid crystal confined to a long capillary and subject to an external magnetic field is studied numerically. Nematodynamic equations are reviewed, followed by an introduction of characteristic scales and short explanation of the numerical implementation. Snapshots of three-dimensional director and velocity fields are presented. It is demonstrated that there are cases, where the backflow does not merely introduce quantitative corrections to the director dynamics, but changes the relaxation process in a complete manner.

1 Introduction

Coupling of the director reorientation and hydrodynamic motion in nematic liquid crystals has been studied mainly in terms of the Ericksen-Leslie continuum theory of the nematic liquid crystal [1,2].

In one-dimensional geometry, switching processes were studied decades ago [3–6]. The instability against periodic distortion in the case of the Freedericksz transition (first observed by Carr [7]) has been studied by Guyon *et al.* [8] for the two-dimensional case, and by Hurd *et al.* [9] for three dimensions. The pattern formation in a rotating magnetic field has been observed experimentally and accounted for numerically by Migler *et al.* [10,11]. An experiment measuring the rotational viscosity is presented by Bajc *et al.* [12], together with a full hydrodynamic numerical treatment in cylindrical geometry (one-dimensional problem).

There has been little or no work done on the backflow problems in severely confined systems. The flow patterns are quite complicated there, since the backflow is actually a consequence of the confinement. To tackle such problems, one usually has to deal with at least two spatial coordinates and vectors in general direction (three velocity components, two independent director components). Together with the pressure, this gives 6 scalar quantities depending on two spatial coordinates to be solved for. The introduction of the second spatial coordinate is particularly involved. Thus, the problem gets very extensive, this being a possible reason for the missing work. In our previous paper [13], we have studied a two-dimensional backflow problem in rectangular cells. It has been shown that depending on the aspect ratio of the cell, the backflow effect can be either pronounced or suppressed, resulting in greater or smaller quantitative corrections. Nevertheless, regions of opposite director rotation have been observed, both in the field-off (known as the *kick-back* effect [14, p. 167]) as well as in the field-on case. This led to an idea of trying to enhance the back-rotation by a suitable magnetic field, and thereby invoke a backflow effect that is not merely a perturbation.

In this paper a full hydrodynamic study of a nematic sample confined to an infinitely long capillary with a square cross section and subject to magnetic field is presented. The aim of the work is to show that in fact there are cases where the backflow can produce more than just small quantitative corrections. In two examples to be demonstrated, the backflow completely alters the dynamics of the switching process.

First a short review of nematodynamic equations is given, followed by an introduction of characteristic scales of the problem. Then the two numerical examples are discussed.

⋆ Author for correspondence: e-mail: daniel@fiz.uni-lj.si

† *In memoriam Frank Mathews Leslie, FRS*

2 Equations of nematodynamics

Three basic equations are involved in the problem of nematodynamics; these are the equation of motion of the director field, the generalized Navier-Stokes equation, and the equation of continuity. The latter is simply reduced to the equation of incompressibility, whereas the former two are relatively extensive due to the (uniaxial) anisotropy of the nematic fluid as well as to the coupling between the director reorientation and flow.

The time evolution equation for the director field is a balance between generalized elastic, electromagnetic and viscous forces. In principle, both electric and magnetic field can be used to manipulate the nematic director. However, the use of electric field, though more efficient, brings about some difficulties to deal with, i.e. the dielectric problem has to be solved exactly, and the convection of ions should be taken into account. As a result of this, the theoretical study to be presented in this paper uses a magnetic field. To obtain the elasto-magnetic part, the Frank elastic free energy density [15, pp. 102, 119] is used:

$$f = \frac{1}{2}K_{11}(\nabla\cdot\mathbf{n})^2 + \frac{1}{2}K_{22}\left[\mathbf{n}\cdot(\nabla\times\mathbf{n})\right]^2 + \frac{1}{2}K_{33}\left[\mathbf{n}\times(\nabla\times\mathbf{n})\right]^2 - \frac{1}{2}\frac{\chi_a}{\mu_0}(\mathbf{n}\cdot\mathbf{B})^2, \tag{1}$$

where $\mathbf{n}$ is a unit vector representing the director, K_{11}, K_{22}, and K_{33} are the splay, twist, and bend elastic constants, respectively, $\mathbf{B}$ is the magnetic field, and χ_a is the magnetic susceptibility anisotropy, i.e. the difference between the susceptibilities parallel and perpendicular to the director. The case of $\chi_a > 0$ will be considered here, as this is the situation present in most nematic substances. The surface terms have been dropped in (1) on account of fixed boundary conditions, corresponding to infinitely strong anchoring.

The Euler-Lagrange equations for the free energy functional

$$F = \int dV\ \left(f(\mathbf{n},\nabla\mathbf{n}) - \lambda(\mathbf{r})\mathbf{n}^2\right) \tag{2}$$

with the constraint $\mathbf{n}^2 = 1$ and f given by (1), give the elasto-magnetic generalized force:

$$h_i^{em} = -\frac{\partial f}{\partial n_i} + \partial_j\left(\frac{\partial f}{\partial(\partial_j n_i)}\right). \tag{3}$$

The equilibrium condition reads

$$\mathbf{h}^{em} = -\lambda(\mathbf{r})\mathbf{n}, \tag{4}$$

where λ is the Lagrange multiplier, i.e. the force $\mathbf{h}^{em}$ must be parallel to $\mathbf{n}$ everywhere. One gets rid of the redundant director degree of freedom and the multiplier by projecting (4) onto the plane perpendicular to the director.

The viscous generalized force is obtained from the dissipation function containing scalar invariants formed with $\mathbf{n}$, $\dot{\mathbf{n}}$, and $\nabla\mathbf{v}$, being bilinear in the latter two [16, p. 142]:

$$\mathbf{h}^v = -\gamma_1\mathbf{N} - \gamma_2\mathsf{A}\cdot\mathbf{n}, \tag{5}$$

where the rotational viscosity γ_1 and γ_2 are expressed in terms of the Leslie viscosity coefficients α_i, $\gamma_1 = \alpha_3 - \alpha_2$, $\gamma_2 = \alpha_3 + \alpha_2$. With $\dot{\mathbf{n}}$ being the material time derivative of the director,

$$\mathbf{N} = \dot{\mathbf{n}} - \frac{1}{2}(\nabla\times\mathbf{v})\times\mathbf{n} = \dot{\mathbf{n}} + \mathsf{W}\cdot\mathbf{n}$$

is the vector of the relative director rotation with respect to the rotation of the fluid, and finally,

$$\mathsf{A}_{ij} = \frac{1}{2}(\partial_i v_j + \partial_j v_i),$$

$$\mathsf{W}_{ij} = \frac{1}{2}(\partial_i v_j - \partial_j v_i)$$

are the symmetric and antisymmetric parts of the velocity gradient, respectively. The viscous force $\mathbf{h}^v$ also needs to be projected to the plane perpendicular to the director.

The equation of motion of the director reads briefly

$$\left\{\mathbf{h}^{em} + \mathbf{h}^v\right\}_{\perp\mathbf{n}} = 0, \tag{6}$$

or in more detail

$$\gamma_1 \frac{\partial \mathbf{n}}{\partial t} = \left\{ \mathbf{h}^{em} - \gamma_2 \mathsf{A} \cdot \mathbf{n} - \gamma_1 \left[\mathsf{W} \cdot \mathbf{n} + (\mathbf{v} \cdot \nabla)\mathbf{n} \right] \right\}_{\perp \mathbf{n}}. \tag{7}$$

The generalized Navier-Stokes equation,

$$\rho \left[\frac{\partial \mathbf{v}}{\partial t} + (\mathbf{v} \cdot \nabla)\mathbf{v} \right] = -\nabla p + \nabla \cdot (\sigma^v + \sigma^e), \tag{8}$$

where ρ is the density, p is the pressure, and the divergence of a tensor defined as $(\nabla \cdot \sigma)_i = \partial_j \sigma_{ji}$, involves two stress tensor contributions. The viscous part is obtained from the same dissipation function as the generalized force (5) [16, p. 142]:

$$\begin{aligned} \sigma^v = {} & \alpha_1 \mathbf{n} \otimes \mathbf{n} (\mathbf{n} \cdot \mathsf{A} \cdot \mathbf{n}) + \alpha_2 \mathbf{n} \otimes \mathbf{N} + \alpha_3 \mathbf{N} \otimes \mathbf{n} + \\ & \alpha_4 \mathsf{A} + \alpha_5 \mathbf{n} \otimes (\mathsf{A} \cdot \mathbf{n}) + \alpha_6 (\mathsf{A} \cdot \mathbf{n}) \otimes \mathbf{n}, \end{aligned} \tag{9}$$

where α_i's are the Leslie viscosity coefficients. The elastic part of the stress tensor is a consequence of deformations changing the director field gradients [15, p. 152]:

$$\sigma^e_{ij} = -\frac{\partial f}{\partial(\partial_i n_k)} \partial_j n_k. \tag{10}$$

The pressure field in (8) is set by the incompressibility condition

$$\nabla \cdot \mathbf{v} = 0, \tag{11}$$

i.e. it has to be determined in such a way that (11) is satisfied.

3 Characteristic scales

The problem involves two length scales: the container size, i.e. the thickness of the capillary L, and the magnetic coherence length

$$\xi_m = \frac{1}{B} \sqrt{\frac{\mu_0 K_{11}}{|\chi_a|}}. \tag{12}$$

In order that field effects be prominent, ξ_m must be small compared with L. Therefore ξ_m is the length relevant for the dynamics of the system.

The director equation of motion (7) and the generalized Navier-Stokes equation (8) introduce a characteristic time scale each. Typical relaxation time of the director field is

$$\tau = \frac{\gamma_1 \xi_m^2}{K_{11}}, \tag{13}$$

if ξ_m is the characteristic length of the director variation. Since the dynamics is governed by the director field relaxation, τ is the characteristic time of the switching process.

The other time scale is given by a typical transition time during which the velocity field is equilibrated to its stationary value due to viscous forces,

$$\tau_0 = \frac{\rho L^2}{\alpha_4}. \tag{14}$$

The isotropic viscosity coefficient α_4 (see (9)) is of the same order of magnitude as the rotational viscosity γ_1, so it is convenient to use the latter in the estimate (15). Typically, the ratio of the two time scales – the unsteadiness parameter – is of the order of

$$\tau_0/\tau = \frac{L^2}{\xi_m^2} \frac{\rho K_{11}}{\gamma_1^2} \approx L^2/\xi_m^2 \cdot 10^{-6}. \tag{15}$$

This means that unless the container size L is much larger than the coherence length, the velocity field is adapted quickly to a given director field and its time derivative, so that during the reorientation process it behaves quasi-stationary – the partial time derivative in (8) can be dropped.

The characteristic magnitude of the velocity can be estimated by equating the viscous force (the α_4 term in (9)) and the viscous force exerted by the director rotation, which drives the flow (the α_2 and α_3 terms in (9)), yielding

$$v_0 = \frac{K_{11}}{\gamma_1 \xi_m} = \xi_m/\tau. \tag{16}$$

As indicated in (16), the same estimate can be obtained in a simpler fashion, although it might not seem as comprehensive. Again it was assumed that $\alpha_4 \approx \alpha_2 \approx \gamma_1$. The characteristic length of the velocity variation is estimated to L. To be more precise, both length scales, L and ξ_m, are intertwined here, but L is used in order to overestimate the Reynolds number:

$$Re = \frac{L}{\xi_m} \frac{\rho K_{11}}{\gamma_1^2} \approx L/\xi_m \cdot 10^{-6}. \tag{17}$$

Unless the magnetic coherence length is tiny in comparison with L, the Reynolds number is much smaller than unity, and the nonlinear advective derivative term in (8) can be dropped. In addition, if the ratio (15) is small as well, also the partial time derivative in (8) can be omitted, as mentioned above. The reader should note that usually the Reynolds number is more than an order of magnitude smaller than the unsteadiness parameter.

4 Description of the problem and numerical implementation

In this paper the relaxation of a nematic sample upon switching a magnetic field is studied. A tube-like geometry is considered: the quantities involved vary across the cross-section of the tube (a square), while there is no dependence in the direction parallel to the long axis. Nevertheless, the components of the vectors are still present in that direction. Infinitely strong anchoring is assumed, which fixes the director field at the boundaries. In practice, this means that the extrapolation length [15, p. 113], ξ, must be much smaller compared both with the sample size and the magnetic coherence length, i.e. $\xi \ll L$ and $\xi \ll \xi_m$. Standard no-slip boundary conditions are prescribed for the flow, setting the velocity to zero at the boundaries.

Material parameters such as the viscosity and the elastic coefficients correspond to those for MBBA, listed in [15, pp. 105, 231]. It is convenient to give some typical magnitudes. A magnetic field with strength 0.1 T gives a coherence length of about 10 μm and the characteristic time (13) of around 2 s. Extrapolation lengths as small as 100 nm or even smaller are readily observed, so that the strong anchoring limit is realistic.

The partial differential equations (7) and (8) are put in a dimensionless form using characteristic scales introduced above. They are solved using finite difference discretisation. The outline of the method is as follows. At a given director field and its time derivative, the generalized Navier-Stokes equation (8) without the advective derivative term is explicitly iterated in time. After that, knowing the velocity field, the director equation (7) is explicitly iterated in time to yield the new director field. Then the velocity is updated again, and so forth. According to the big difference in characteristic time scales (14) and (13), one makes many iterations of (8) before updating the director field. For a generic set of material parameters the unsteadiness parameter (15) is small enough, so one could drop the time derivative term in (8) in the first place. However, with the explicit iterative numerical scheme described above this has little sense. On the other hand, (8) without the nonlinear term and (11) together result in a large set of linear equations for the discretized velocity and pressure variables, which can be solved directly for the stationary velocity field. In practice it turned out that the iterative method is far more efficient. The velocity and pressure variables are discretized on a staggered grid [17, p. 331] in order to prevent the occurrence of the well-known oscillatory pressure solution. The incompressibility condition is satisfied in a standard way by solving a Poisson equation for pressure corrections at every velocity iteration step [17, p. 340]. At the boundaries, normal pressure correction derivatives are specified in order to meet the incompressibility condition there. The calculations were typically done on a square mesh of size 60 x 60.

5 Calculated examples

Two switching examples have been chosen to demonstrate the role of the backflow in relaxation processes. The nematic sample is confined to an infinitely long capillary of square cross section. The domain of calculation

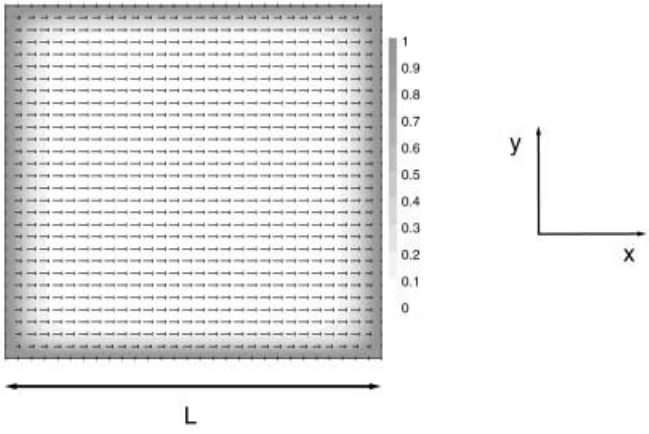

Fig. 1. The initial director field configuration. Shading (although redundant in the case of the director field) represents the out-of-plane (z) component, while the in-plane components are drawn as nails as customary. Magnetic field with coherence length of $L/30$ is applied in the x direction

corresponds to the cross-section (a square in the xy plane) and is thus two-dimensional. The anchoring is infinitely strong, its direction is parallel to the tube axis (z axis). Initial conditions are identical in both cases: the sample is aligned by an in-plane magnetic field with the coherence length (12) of $1/30$ of the tube thickness L, pointing along the x axis (Fig. 1). Following the discussion in Sects. 3 and 4, for a 100 μm thick capillary the corresponding field is around 0.3 T, and the characteristic time (13) is about 0.2 s.

The switching process is started by suddenly rotating the magnetic field to a perpendicular direction. The switching time of the field must be short compared with the characteristic time (13). In the first example, the final field is parallel to the tube axis, whereas in the second example, it lies in the yz plane at an angle 70° with respect to the z axis. It will be shown that due to the backflow, the switching process is altered completely. One should mention that a similar phenomenon to the one shown in the first example can be studied also in a simpler two-dimensional geometry, like the square in [13]. Nevertheless, to relate it to the second example, and above all, to make a step toward possible experimental set-ups, the more demanding tube-like geometry has been chosen.

A. Example 1

After the magnetic field has been switched to the z direction, near the boundary the director is rotated out of the plane by elastic and field torques. On the other hand, the elastic and field torques are almost zero in the center. If one disregards the backflow, the director will align with the new field by a clockwise rotation about the y axis, proceeding from the boundary toward the center.

The backflow, however, can produce a large effect in this case, since the director orientation in the central region is labile with respect to the field, and thus quite sensible to perturbations. The rate of director rotation has two minima – at the boundary and in the center, and a maximum inbetween. As a result of this, an out-of-plane fluid flow is generated (Fig. 2, (a)), where the velocity changes sign three-times as we move along x direction, whereas on passing along y it is single-signed. The mechanisms governing this phenomenon are explained in [13]. The flow rotates the director in the center in the opposite direction than expected (the *kick-back* effect). This rotation is amplified by the magnetic field. Thus, we are left with the center rotating in the opposite direction as the outer part of the sample, which leads to the formation of a domain (Fig. 2, (b)). The width of the domain wall is characterized by the magnetic coherence length. Once the domain is formed it begins to shrink (Fig. 2, (c)), which is a slow process compared with the formation, driven by the domain wall curvature[18, p. 213]. Neglecting the flow and the elastic anisotropy, the shrinking rate of a thin circular domain with radius R scales as $dR/dt \propto -1/R$, if R and t are expressed in dimensionless units $R \to R/\xi_m$ and $t \to t/\tau$, respectively. This gives the shrinking time $t \propto R^2(0)$, with $R(0)$ being the initial radius of the domain. For $R(0) = L/4\xi_m = 30/4$ a rough estimate for the shrinking time is $t \approx 50$, or 50τ in physical units. On the other hand, the characteristic time for the formation of the domain is just τ.

B. Example 2

In order to show that the effect is not limited only to a certain direction of the final magnetic field, a second example is to be demonstrated. The initial configuration is the same as in the previous case (Fig. 1), but now the final field is in the yz plane at an angle 70° with respect to the z axis. It is important that the initial and the final

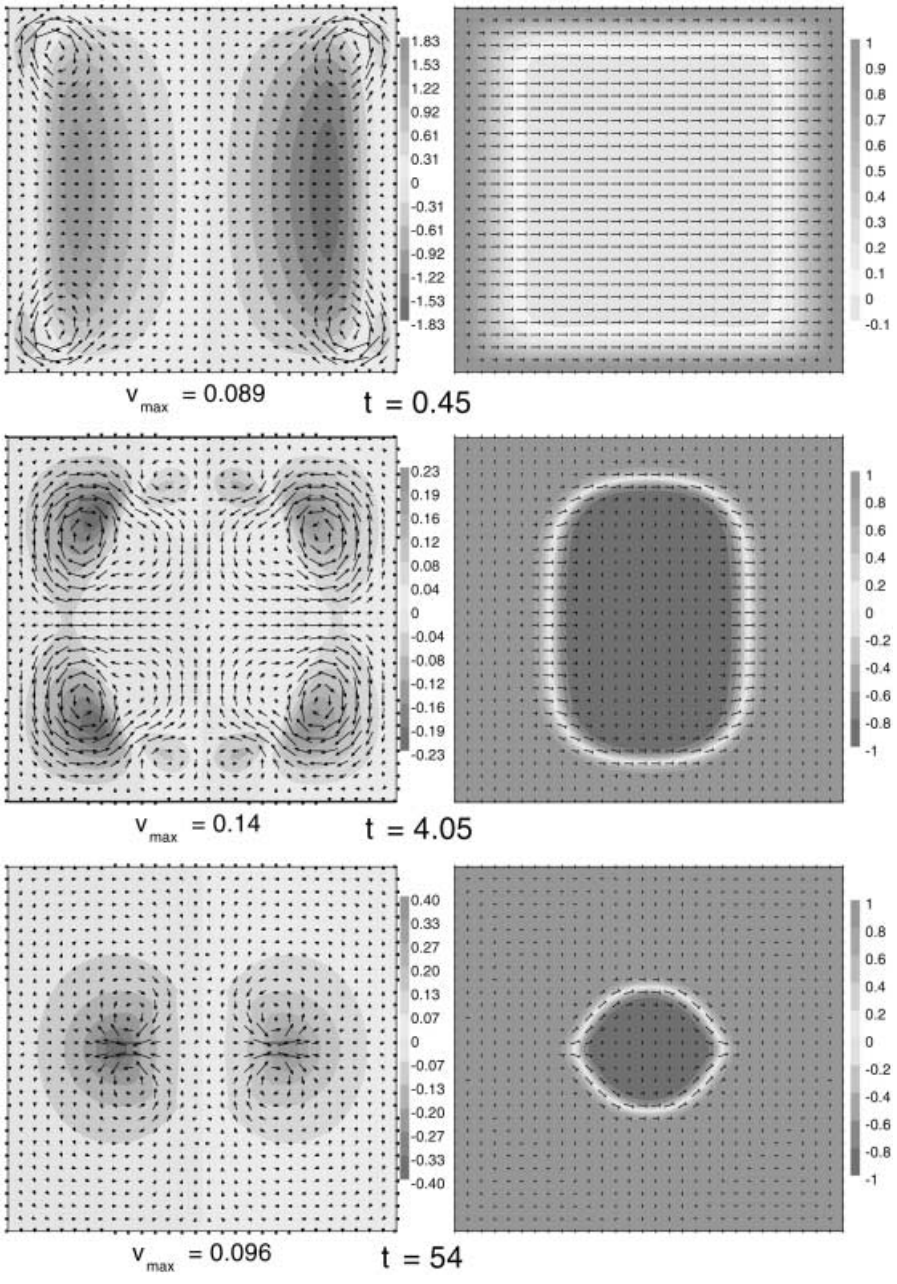

Fig. 2. Example 1: velocity (*left column*) and director fields (*right column*) in selected moments of time (in units of τ as defined in (13)). The number of mesh points displayed has been reduced by a factor of two in each direction to gain clarity. Key to the figures is given with Fig. 1. Light grey and dark grey levels represent components up and down, respectively. The maximum magnitude of the in-plane velocity is denoted v_{max}. The velocities are given in units of v_0 as defined in (16). The reader should be careful not to confuse the heads of nails with the nails themselves, where the directors point almost in the z direction. (a) The kick-back caused by the out-of-plane flow. (b) The kick-back is amplified by the magnetic field, a domain is formed. (c) As the domain shrinks, a major part of the domain wall becomes a twist wall due to the elastic anisotropy: K_{11} and K_{33} are about twice as large as K_{22}.

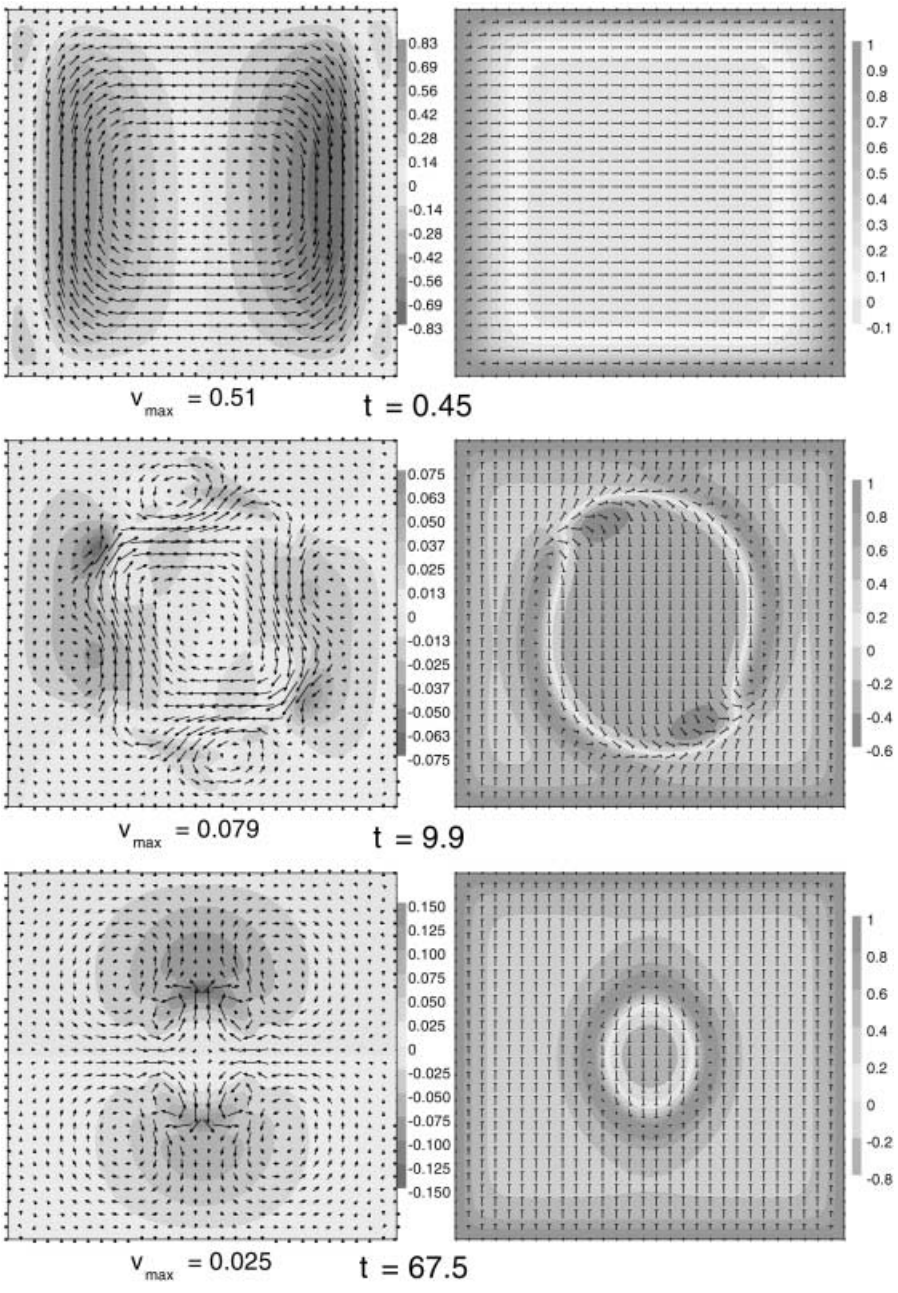

Fig. 3. Example 2: velocity (left column) and director fields (right column) in selected moments of time. The number of mesh points displayed has been reduced by a factor of two in each direction to gain clarity. Key to the figures is given with Figs. 5 and 2. (a) Both the out-of-plane and in-plane flow velocities are comparable in magnitude, resulting in the kick-back around an oblique axis. (b) A part of the splay-bend domain wall first created (not shown) is transformed to a twist wall due to the elastic anisotropy, resulting in a complex wall structure. (c) As the domain shrinks, the structure of the wall becomes simpler.

field are still perpendicular to each other, or close enough to this, i.e. a few degrees. If not so, the field torque outweighs the backflow-generated one even in the beginning, and the backflow can give only quantitative effects. The situation is similar as in the previous example, only that now the flow is both out-of-plane and in-plane and the domain wall is more complex (Fig. 3).

It is worth mentioning that if the final field is too close to the cross-section plane (a few degrees), even in the absence of the flow the director rotation is complicated by the elastic anisotropy. Namely, due to the anisotropy, the director deviates slightly from the x direction initially, which causes the director to rotate in opposite directions in different parts of the sample. Despite the backflow is important in this case also, we do not aim to give examples, since they are too complicated and thus not particularly instructive.

6 Conclusion

In this paper, nematodynamic problems have been studied in the geometry of an infinitely long capillary with a square cross section, making no approximation other than omitting the nonlinear term in (8), which is reasonable for the problems concerned. It has been shown by two specific examples that there are cases where the backflow effect is crucial. If in a part of the sample the director is near an unstable equilibrium with respect to the field, the backflow usually produces a perturbation strong enough to change the director rotation in that part. Of course, only those cases are interesting, where the backflow has a frustrating influence on the director field, i.e. it creates regions of opposite director rotation. In [13], such relaxation processes have been referred to as the two-step processes, as opposed to the one-step processes, where backflow is less important.

Infinitely strong anchoring has been assumed. In order to observe any relevant backflow effects in practice, the anchoring should be strong enough ($\xi/\xi_m \ll 1$), which can be readily achieved in experiments. Numerical evidence for the ceasing backflow effect in the case of finite anchoring has been given toward the end of [19]. Disregarding any surface viscosity effects, one can make a simple estimate for the case when the anchoring becomes finite, $\xi > 0$, but remains strong, $\xi/\xi_m \ll 1$. Comparing the director profiles near the boundary for the infinite and the finite anchoring in the presence of the magnetic field, one finds the director gradient to decay as $\xi_m/(\xi_m + \xi) \approx 1 - \xi/\xi_m$. Upon removal of the field (or, in the examples given, rotating the field into a perpendicular direction), the director is rotated by elastic forces ((7)), decaying as $\xi_m^2/(\xi_m + \xi)^2 \approx 1 - 2\xi/\xi_m$. It then follows that the divergence of the α_2 and α_3 terms in (9), which represents the source driving the flow in (8), decays as $1 - 3\xi/\xi_m$ as the anchoring gets weaker. Hence, the magnitude of the backflow and its torque exerted on the director ((7)) decay the same way.

As indicated by additional calculations not presented in this paper, the qualitative picture does not depend on the exact geometry of the tube cross section, i.e. the square could be replaced by a circle or a rectangle, etc., provided that the aspect ratio stays roughly the same. Also, the detailed structure of the domain wall appears to depend on the ratio of the elastic constants, as mentioned in captions to the Figs. 2 and 3.

It is worth pointing out again that the complexity of the velocity patterns has nothing to do with any kind of turbulence, since the Reynolds number is tiny and the nonlinear term in (8) has been dropped. It is merely a consequence of the complicated coupling to the director field, given by (9) and (10).

Besides specific examples of this kind, there is another type of problems where the backflow is expected to be very important, namely the relaxation of structures containing defects, e.g. attraction of defects, defect annihilation, etc.

Acknowledgements. This work was supported by the Slovenian Office of Science (Program P0-0503-1554), US-Slovene NSF Joint Found (Grant No. 9815313), and SILC TMR ERBFMRX-CT98-0209 project.

References

1. Ericksen JL (1960) *Arch. ration. Mech. Analysis* 4, 231.
2. Leslie FM (1966) *Quart. J. Mech. appl. Math.* 19, 357; 1968, *Arch. ration. Mech. Analysis* 28, 265
3. Clark MG, Leslie FM (1978) *Proc. R. Soc. Lond. A.* 361, 463
4. Van Doorn CZ (1975) *J. Physique* 36, C1–261
5. Brochard F, Pieranski P, Guyon E (1972) *Phys. Rev. Lett.* 26, 1681
6. Pieranski P, Brochard F, Guyon E (1973) *J. Physique* 34, 35
7. Carr EF (1977) *Mol. Cryst. Liq. Cryst.* 34, 159
8. Guyon E, Meyer R, Salan J (1979) *Mol. Cryst. Liq. Cryst.* 54, 261
9. Hurd AJ, Fraden S, Lonberg F, Meyer RB (1985) *J. Physique* 46, 905

10. Migler K, Meyer R (1991) *Phys. Rev. Lett.* 66, 1485
11. Migler K, Meyer R (1993) *Phys. Rev. E* 48, 1218
12. Bajc J, Hillig G, Saupe A (1997) *J. Chem. Phys.* 106, 7372
13. Svenšek D, Žumer S (2001) *Liq. Cryst.* 28(9), 1389
14. Chandrasekhar S (1992) *Liquid Crystals.* Cambridge: Cambridge University Press
15. De Gennes PG, Prost J (1995) *The Physics of Liquid Crystals.* Oxford: Clarendon Press
16. Vertogen G, De Jeu WH (1988) *Thermotropic Liquid Crystals, Fundamentals.* Berlin: Springer-Verlag
17. Fletcher CAJ (1988) *Computational Techniques for Fluid Dynamics*, Volume II. Berlin: Springer-Verlag
18. Bray A J (2000) In: *Soft and Fragile Matter.* Proceedings of the 53rd SUSP, St. Andrews, July 1999, edited by M. E. Cates and M. R. Evans (The Scottish Universities Summer School in Physics)
19. McIntosh JG, Leslie FM (2000) *J. Eng. Math.* 37, 129